Virologica Sinica 40 (2025) 349–360

Contents lists available at ScienceDirect

Virologica Sinica

journal homepage: www.keaipublishing.com/en/journals/virologica-sinica
www.virosin.org

Research Article

Characterization of a SARS-CoV-2 infection model in golden hamsters with diabetes mellitus

Hao-Feng Lin [a,1], Ren-Di Jiang [c,1], Rui-Xin Qin [b,1], Bing Yao [d], Wen-Tao Zeng [b], Yun Gao [b,*], Ai-Min Shi [b,*], Jian-Min Li [b,*], Mei-Qin Liu [a,*]

[a] The First Affiliated Hospital of Guangzhou Medical University, Guangzhou Laboratory Clinical Base, State Key Laboratory of Respiratory Disease, Guangzhou Medical University, Guangzhou, 510120, China
[b] State Key Laboratory of Reproductive Medicine and Offspring Health, Jiangsu Laboratory Animal Center, Jiangsu Animal Experimental Center of Medicine and Pharmacy, Department of Cell Biology, Animal Core facility, Key Laboratory of Model Animal, Collaborative Innovation Center for Cardiovascular Disease Translational Medicine, National Vaccine Innovation Platform, Nanjing Medical University, Nanjing, 211166, China
[c] State Key Laboratory of Genetic Engineering, Greater Bay Area Institute of Precision Medicine (Guangzhou), School of Life Sciences, Zhongshan Hospital, Fudan University, Shanghai, 200433, China
[d] Jinling Hospital Department Reproductive Medical Center, Nanjing Medical University, Nanjing, 211166, China

ARTICLE INFO

Keywords:
Severe acute respiratory syndrome coronavirus 2 (SARS-CoV-2)
Diabetes
Hamster
Pneumonia
Multiorgan injury

ABSTRACT

Being widespread across the globe, severe acute respiratory syndrome coronavirus 2 (SARS-CoV-2) keeps evolving and generating new variants and continuously poses threat to public health, especially to the population with chronic comorbidities. Diabetes mellitus is one of high-risk factors for severe outcome of coronavirus disease 2019 (COVID-19). Establishment of animal models that parallel the clinical and pathological features of COVID-19 complicated with diabetes is thus highly essential. Here, in this study, we constructed leptin receptor gene knockout hamsters with the phenotype of diabetes mellitus (db/db), and revealed that the diabetic hamsters were more susceptible to SARS-CoV-2 and its variants than wild-type hamsters. SARS-CoV-2 and its variants induced a stronger immune cytokine response in the lungs of diabetic hamsters than in wild-type hamsters. Comparative histopathology analyses also showed that infection of SARS-CoV-2 and the variants caused more severe lung tissue injury in diabetic hamsters, and may induce serious complications such as diabetic kidney disease and cardiac lesions. Our findings demonstrated that despite the decreased respiratory pathogenicity, the SARS-CoV-2 variants were still capable of impairing other organs such as kidney and heart in diabetic hamsters, suggesting that the risk of evolving SARS-CoV-2 variants to diabetic patients should never be neglected. This hamster model may help better understand the pathogenesis mechanism of severe COVID-19 in patients with diabetes. It will also aid in development and testing of effective therapeutics and prophylactic treatments against SARS-CoV-2 variants among these high-risk populations.

INTRODUCTION

Coronavirus disease 2019 (COVID-19) is an acute respiratory illness with high contagiousness (Zhu et al., 2020). It led to one of the most serious worldwide pandemics in human history and severely challenged global public health (https://covid19.who.int/). The causative agent of COVID-19, severe acute respiratory syndrome coronavirus 2 (SARS-CoV-2) (Coronaviridae Study Group of the International Committee on Taxonomy Of virus, 2020; Zhou et al., 2020), is prone to genomic variation. With the continuous mutation of the SARS-CoV-2 in the context of the pandemic, novel variants of concern (VOCs) of SARS-CoV-2 have been emerging including Alpha (Davies et al., 2021a, 2021b) (B.1.1.7), Beta (Tegally et al., 2021) (B.1.351), Gamma (Faria et al., 2021) (P.1), Delta (Li B. et al., 2022) (B.1.617.2), as well as the Omicron variants (Liu Y. and Rocklov, 2022) which have been the predominant strains since early 2022. In recent years, the ongoing evolution of SARS-CoV-2 have generated more sub-lineages of

* Corresponding authors.
E-mail addresses: 2023390024@gzhmu.edu.cn (M.-Q. Liu), jianminlilab@njmu.edu.cn (J.-M. Li), sam@njmu.edu.cn (A.-M. Shi), yun@njmu.edu.cn (Y. Gao).
[1] Hao-Feng Lin, Ren-Di Jiang, and Rui-Xin Qin contributed equally to this work.

https://doi.org/10.1016/j.virs.2025.05.001
Received 23 November 2024; Accepted 12 May 2025
Available online 17 May 2025

Omicron variants such as JN.1, XBB1.5, B.Q.1.1 (Looi, 2023; Wang et al., 2024). These novel variants have higher infectivity, transmissibility, and immune evasion capacity compared to the SARS-CoV-2 prototype strain (Hachmann et al., 2022; Liu and Rocklov, 2022). The altered antigenic properties, virulence, as well as the limited time duration of immunity established in populations after vaccination or infection, may result in breakthrough infections by the new SARS-CoV-2 variant (Cao et al., 2023; Li et al., 2024). Therefore, COVID-19 is likely to become a periodically recurrent disease and coexist with humans for long time.

Diabetes mellitus is recognized as one of the risk factors for adverse outcomes of various viral infection diseases. During the SARS-CoV outbreak in 2002–2003, type 2 diabetes mellitus (T2DM) was identified as an independent risk factor for death (Yang et al., 2006). In the H1N1 influenza pandemic in 2009, the admission rate of intensive care unit (ICU) among patients with T2DM was up to four times compared with the general populations (Allard et al., 2010). For Middle-East respiratory syndrome (MERS) patients, those with T2DM had a significantly higher chance of developing critical illness than the general populations (Alraddadi et al., 2016). Multiple epidemiological studies suggested that manifestation and severity of COVID-19 was associated with some risk factors including several chronic comorbidities such as diabetes, obesity, cardiovascular disease, etc. Available clinical data suggest that either type 1 diabetes mellitus (T1DM) or T2DM is among the high-risk factors for severe COVID-19 (Wang et al., 2020; Singh and Khunti, 2022). A whole-population study conducted in UK revealed that patients with diabetes had a higher risk of COVID-19-associated death than non-diabetic cases (Barron et al., 2020). It was reported that one-third of COVID-19 death in England from March 1st to May 11th' 2020 occurred in diabetic patients (Barron et al., 2020). According to the International Diabetes Federation, approximately 10 % of the world's population had diabetes in 2021, and this number is steadily increasing (http://www.diabetesatlas.org/). Considering the large diabetic populations in the worldwide scale, although the pathogenicity of novel Omicron variants is milder than the prototype SARS-CoV-2 strain, the disease severity of COVID-19 in diabetic patients should never be ignored.

Leptin plays a key role in the metabolism and regulation of blood glucose levels (D'souza A et al., 2017). Mice are the most commonly used animal model for diseases researches, and the leptin receptor-deficient mice have been widely used as a standard animal model in the studies of T2DM (Chen et al., 1996; Oliveira et al., 2022; Gogiraju et al., 2023). However, since SARS-CoV-2 does not efficiently bind to mouse ACE2, wild-type mice are not highly susceptible to SARS-CoV-2 infection (Gu et al., 2020; Jiang et al., 2020; Huang et al., 2021; Sun et al., 2021). In contrast, the spike of SARS-CoV-2 shows high binding affinity to the ACE2 receptor of Syrian golden hamster. It can efficiently replicate in lungs of hamsters and result in respiratory disease and lung lesions that resemble those observed in COVID-19 patients with pneumonia, making this animal an important model for studying COVID-19 (Imai et al., 2020; Sia et al., 2020). Hence, the leptin receptor knockout hamsters (db/db hamsters) may serve as an ideal animal model for studying SARS-CoV-2 infection complicated with diabetes. Given the concurrent threats posed by evolving SARS-CoV-2 variants and the growing morbidity rate of diabetes, there is a strong need to utilize such infection model to assess the risk of disease severity in diabetic patients infected with newly emerging SARS-CoV-2 variants. Moreover, development of a diabetic hamster model that can replicate diabetes-related COVID-19 diseases in humans is an essential prerequisite for investigating the pathogenesis of severe COVID-19 as well as for evaluating the effectiveness of therapeutics and prophylactics among these high-risk populations.

RESULTS

Establishment and validation of the db/db hamster model

Using CRISPR-Cas9 genetic engineering technology, we constructed leptin receptor gene knockout hamsters with the phenotype of diabetes mellitus (db/db), in which the expression leptin receptor is deficient due to a deletion of 16 nucleotides in the exon of leptin receptor gene (Fig. 1A). We collected subcutaneous inguinal adipose tissue of db/db hamsters and wild-type hamsters, and performed Western blot test. No expression of leptin receptor was detected in db/db hamsters, indicating that the db/db hamster model was successfully established (Fig. 1B). Weight monitoring results showed that db/db hamsters had more significant weight increase than wild-type (WT) hamsters under condition of normal feeding, no matter for male or female hamsters, which is similar to the manifestation of T2DM caused by obesity (Fig. 1C). We measured plasma glucose concentrations at various time points following a 16-h fasting period in db/db and WT hamsters, and observed that db/db hamsters exhibited significantly elevated blood glucose levels compared to their wild-type counterparts. This finding aligns with the characteristic of T2DM patients, who are unable to restore blood glucose levels to the normal range without exogenous interventions (Fig. 1D).

db/db hamsters are highly susceptible to SARS-CoV-2 variants

Six-to-ten-week-old db/db or wild-type hamsters were intranasally inoculated with 1×10^5 median tissue culture infectious dose ($TCID_{50}$) of SARS-CoV-2 prototype, Delta, Omicron BA.5 strains or Dulbecco's modified Eagle's medium (DMEM) as control over a 14-day time course (Fig. 2A). For each type of hamsters, two experimental groups were established for each virus: one group was monitored for weight changes and survival rates, while the other group was for tissue sampling at various time points after infection. In the db/db hamsters, approximately 5 % weight loss was observed within 7 days post inoculation (DPI), and the body weight gradually returned thereafter (Fig. 2B). In contrast, wild-type hamsters infected with different SARS-CoV-2 variants did not show weight loss compared to the mock group, except for a relatively slow rate of weight gain in the first seven DPI (Fig. 2C), but the body weight increased rapidly from day 8. No difference was observed among db/db hamsters infected with different variants in terms of body weight change. No animal died in either of the two hamster model groups.

We further investigated the *in vivo* replication of different SARS-CoV-2 variants in db/db and wild-type hamsters. Hamsters were euthanized and tissue samples of liver, lung, kidney and turbinate were collected for virus titer testing at 2, 5, or 14 DPI. Both SARS-CoV-2 and its two variants can effectively replicate in lung tissues of wild-type and db/db hamsters (Fig. 2D). The viral titers decreased gradually over time, and no virus could be detected in either model at 14 DPI. However, the db/db hamsters were more susceptible to infection of SARS-CoV-2 and its variants. At 5 DPI, SARS-CoV-2 and variants still maintained high levels of replication in the lungs of db/db hamsters, while the viral titers drastically decreased (2–6 log values) as compared with 2 DPI in wild-type hamsters, and titers of the Omicron BA.5 variant even cannot be detected. Similarly, in the turbinate tissues, the viral titers of SARS-CoV-2 and its variants decreased gradually over time and was eventually clear (Fig. 2E). In db/db hamsters, clearance of the virus appeared to be slower than in wild-type hamsters. At 5 DPI, the viral titers of SARS-CoV-2 and its variants only slightly decreased in turbinate tissues of db/db hamsters. High level of virus replication can still be detected in two db/db hamsters even at 14 DPI. However, in wild-type hamsters, the titers of the three viruses significantly decreased and some can hardly be detected at 5 DPI. It is noteworthy that in both the wild-type and db/db hamster models, the replication ability of the two SARS-CoV-2 variants is significantly lower than that of the prototype strain in lungs and nasal turbinate tissues, two important target organs of SARS-CoV-2 in lower and upper respiratory tract, respectively. Among the variants, the replication capacity of Omicron BA.5 was weaker than that of Delta. These results were consistent with previous findings that the respiratory pathogenicity of SARS-CoV-2 appears to have gradually reduced after its ongoing mutations within populations (Chan et al., 2022; Shuai et al., 2022, 2023; Carabelli et al., 2023; Puhach et al., 2023; Hu et al., 2024). Furthermore, despite previous reports that SARS-CoV-2 may cause damage to kidney

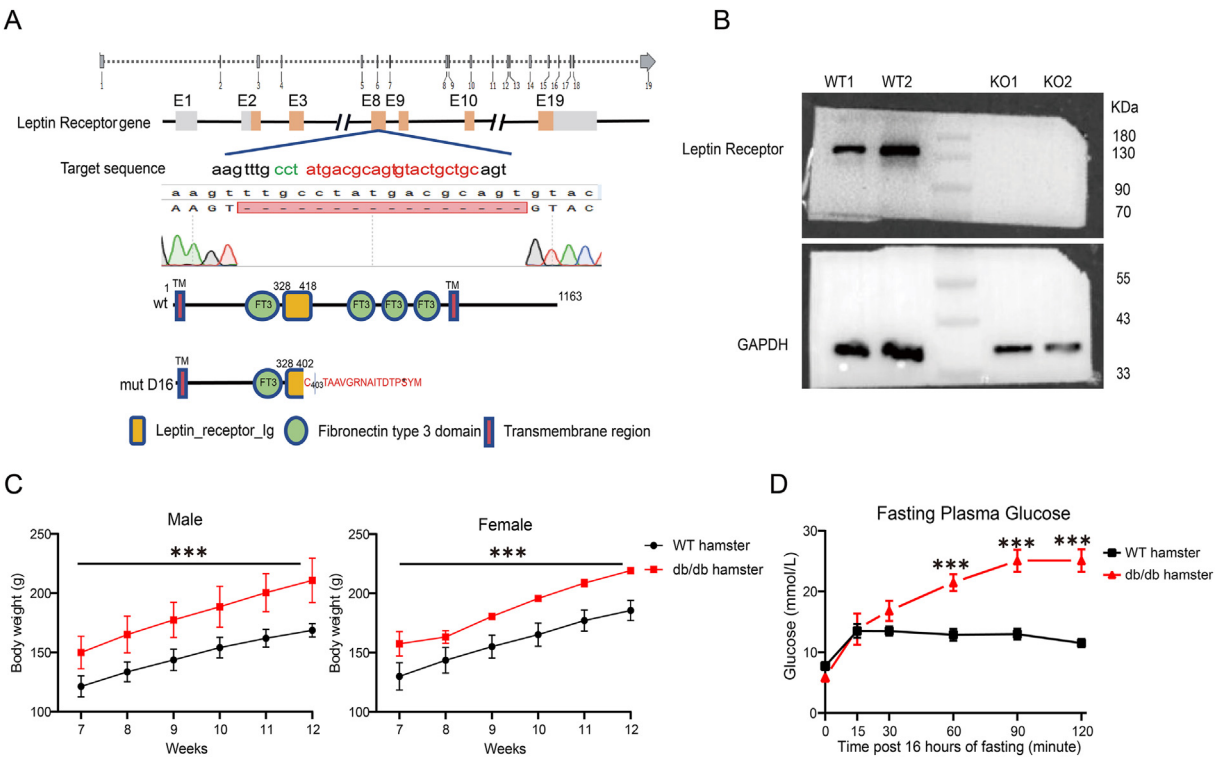

Fig. 1. Strategy for production of the leptin receptor-deficient golden hamsters by CRISPR/Cas9. **A** Structure of the golden hamster leptin receptor gene and target locus for sgRNA. Sequencing result showed 16 nucleotides deletion (mut16) in the leptin receptor-deficient (db/db) golden hamster lines, which resulted in leptin receptor protein mistranslation. **B** Western blots showed the loss of leptin receptor expression in subcutaneous inguinal adipose tissue of db/db hamsters. GAPDH was used as the loading control. **C** Under normal feeding conditions, including feeding with commercial common hamster food, identical rearing environments and feeding frequencies, the body weights of 7–12-week-old db/db hamsters (n = 5) and WT hamsters (n = 5) were routinely monitored. **D** Blood samples were collected from db/db hamsters (n = 5, 2 males, 3 females) and WT hamsters (n = 5, 2 males, 3 females) at various time points following a 16-h fasting period to monitor glucose levels. Error bars indicated the standard error. Statistical significance was measured by two-way ANOVA with multi-comparison model. *** $P < 0.001$.

and liver, we found viable viruses in these two tissues in neither of the hamster model (Kronbichler et al., 2020; Puelles et al., 2020; Diao et al., 2021) (Supplementary Fig. S1A).

SARS-CoV-2 infection induced more severe immune response in db/db hamsters

The severe outcome of COVID-19 could be associated to the inflammation driven by the immune cytokine storm triggered by SARS-CoV-2 infection. A significant rise of inflammatory cytokines such as IL-2, IL-6, IL-7, IL-10 and TNF-α were observed in COVID-19 patients (Chen T. et al., 2020; Liu et al., 2020). We collected the lung tissues of db/db hamsters and wild-type hamsters infected with SARS-CoV-2 and its variants at 5 DPI, and performed testing of inflammatory cytokines (Fig. 3A). Our results showed that SARS-CoV-2 and the variants induced strong immune response in both db/db hamsters and wild-type hamsters, but the inflammatory cytokine response was more intense in db/db hamsters than in wild-type hamsters, including IL-4, IL-10, Cxcl9, Cxcl10, Cc15, and IL-1β. Compared with the prototype strain and the Delta variant, the immune response triggered by BA.5 in db/db hamsters were relatively weak, which was consistent with its lower pathogenicity in general populations and *in vivo* studies in mouse models (Halfmann et al., 2022; Rangu et al., 2022; Carabelli et al., 2023). Despite the milder immune storm induced by the variant, the level of those inflammatory cytokines remained much higher in db/db hamsters than in wild-type hamsters.

Blood biochemical indices are important clinical indicators for disease progression and can assist clinicians to make treatment strategies (Chen N.S. et al., 2020; Huang et al., 2020). We collected serum samples from db/db hamsters and wild-type hamsters at different time points after SARS-CoV-2 infection and tested some clinical blood biochemical indices (Fig. 3B). The results were generally in accordance with previous clinical data in humans. When wild-type hamsters were infected with SARS-CoV-2 and the variants, its blood glucose level (GLU) increased and progressively rose up with infection time. Previous studies found that SARS-CoV-2 can directly infect pancreatic β cells and caused damage, thus reducing insulin secretion (Tang et al., 2021; Wu et al., 2021). We did not detect significant difference in blood glucose levels among groups of different SARS-CoV-2 strains. For db/db hamsters, whose blood glucose were substantially higher than wild-type hamsters, a decrease of blood glucose was observed in the first 5 days after infection, which can likely be explained by the loss of appetite and lethargy caused by infection. Meanwhile, we tested blood urea nitrogen (BUN), alanine aminotransferase (ALT), cholesterol (CHOL), lipase (LIPA), total protein (TP), creatine kinase (CK), and lactate dehydrogenase (LDH) in the infected hamsters. The results showed that the ALT level was abnormally enhanced in Delta-infecting db/db hamsters at 2 DPI, and the CHOL in db/db hamsters are relatively low when infected with SARS-CoV-2 and the variants, as compared with the mock group, indicating liver function injury. In addition, there was a prominent increase of LIPA in db/db hamsters at 2 DPI, which may suggest kidney function injury associated with SARS-CoV-2 infection.

SARS-CoV-2 infection caused more severe multi-organ injury in db/db hamsters

Lung is one of the major target organs of SARS-CoV-2. Lung dysfunction in severe and critical patients of COVID-19 may lead to acute respiratory distress syndrome (ARDS), and even result in lethal disease outcome (Santus et al., 2020; Wang et al., 2020). To examine whether diabetes mellitus can worsen the severity of COVID-19, we sampled lung tissues of db/db hamsters (Fig. 4A) and wild-type hamsters (Fig. 4B) infected with SARS-CoV-2 and its variants at different time points, and

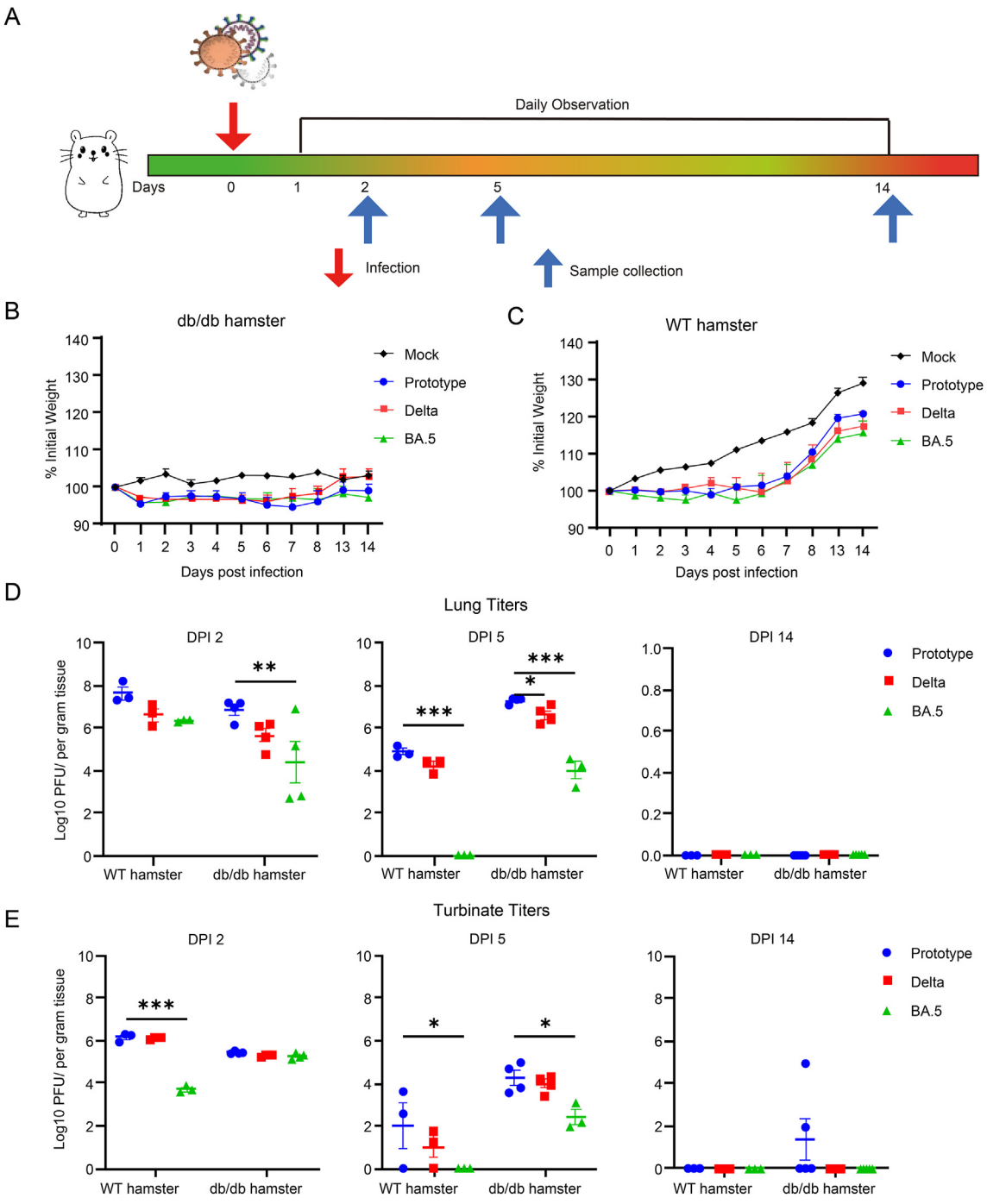

Fig. 2. db/db hamsters are highly susceptible to SARS-CoV-2 variants. Hamsters were divided into two groups, one for monitoring weight change and the survival rate, and the other for tissue sampling at various time points after infection. In the tissue sampling group, six-to-ten-week-old male and female db/db hamsters or wild-type (WT) hamsters were mock-infected or intranasally infected with 1×10^5 $TCID_{50}$ of SARS-CoV-2 prototype, SARS-CoV-2 Delta variant, or SARS-CoV-2 Omicron BA.5 variant, and the infected hamsters were sacrificed for tissue collection at 2, 5, and 14 DPI. **A** Scheme of animal infection. **B, C** For the survival monitoring, body weight and survival of db/db hamsters and wild-type hamsters were monitored daily until 14 DPI after challenge with either DMEM (Mock, 1 male and 2 females) or different SARS-CoV-2 strains (2 males and 3 females). **D, E** For tissue collection of the lung and turbinate at 2, 5, and 14 DPI, virus-infected db/db hamsters (6 males and 7 females for each strain) and WT hamsters (5 males and 4 females for each strain) were euthanized, with both male and female animals included at each sampling time point. Viral load in lung and turbinate of the infected WT and db/db hamsters were detected by plaque formation assay. Error bars indicate the standard error. Statistical significance was measured by two-way ANOVA with multi-comparison model. $^*P < 0.05$, $^{**}P < 0.01$, $^{***}P < 0.001$.

evaluated the lung histopathological changes. The results showed that the lung tissue injury after SARS-CoV-2 or variant infection was reversible in both wild-type and diabetic hamsters. At 2 DPI, hamster lungs displayed local inflammation (black arrows), such as alveolar wall thickening, widening of alveolar space, as well as mild exudation and infiltration of inflammatory cells (green arrows). As the lung tissue structure was damaged because of continuous high level of virus replication, the lung function was transiently impaired. Hematoxylin and Eosin (H&E) staining showed severe pathological injury in hamster lungs at 5 DPI. The characteristic changes included severe thickening of alveolar walls, unclear alveolar structure, necrosis, and exfoliation of bronchial epithelial cells (orange arrows), perivascular edema and infiltration

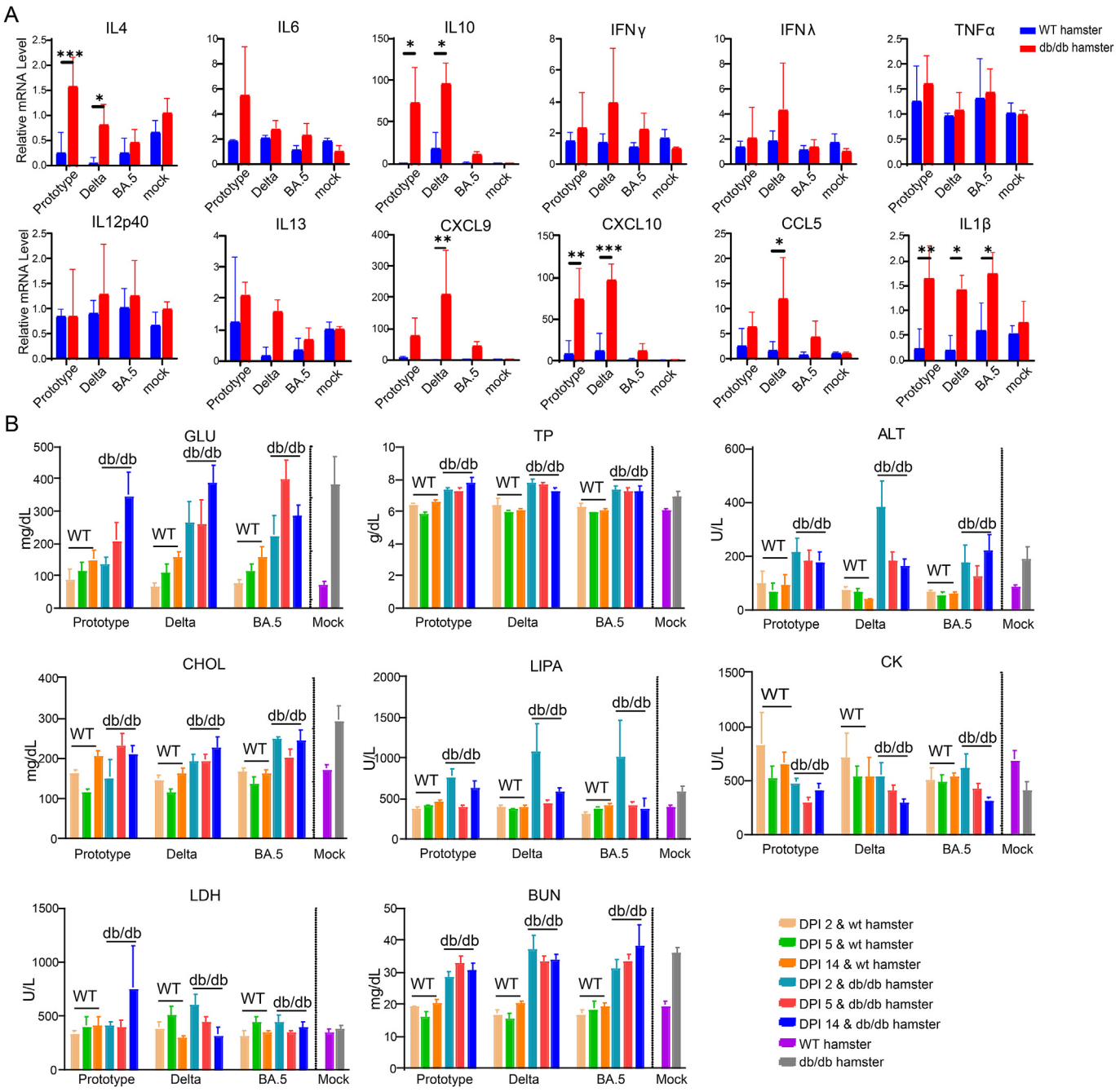

Fig. 3. Testing of clinical blood biochemical indices and immune response in WT and db/db hamsters infected with SARS-CoV-2 variants. Six-to-ten-week-old male and female WT hamsters and db/db hamsters infected with 1×10^5 $TCID_{50}$ of SARS-CoV-2 prototype, SARS-CoV-2 Delta strain, or SARS-CoV-2 Omicron BA.5 strains, and then they were sacrificed for blood and lung tissue collection at 2, 5, and 14 DPI. **A** Cytokine and chemokine from infected-hamsters lung lysates at 5 DPI was quantified by qPCR. **B** Serum samples from infected hamsters at different time points were tested for some clinical blood biochemical indices. Error bars indicate the standard error. Statistical significance was measured by two-way ANOVA with multi-comparison model. $^*P < 0.05$, $^{**}P < 0.01$, $^{***}P < 0.001$.

of a large amount of lymphocytes (green arrows). With the deceased viral load and clearance of virus, the lung injury was gradually improved and recovered, and only local mild inflammation was present at 14 DPI. Generally, db/db hamsters exhibited more severe lymphocytic and granulocytic infiltration and bronchial epithelial cell necrosis than wild-type hamsters, presenting higher pathological scores. Our data suggested that diabetes may contribute to the inflammation and lung pathological injury and induce more serious disease in SARS-CoV-2-infected hamsters, which was consistent with clinical findings that diabetes are high-risk factors of severe COVID-19 and previous results from diabetic mice (Singh and Khunti, 2022; Huang et al., 2023). According to the histopathology scoring system that we previously used (Lin et al., 2023; Mao et al., 2024), the degree of lung injury caused by SARS-CoV-2 variants is weaker than that of the prototype strain (prototype > Detla > Omicron BA.5), which was in line with the results of virus load quantification in lung tissue.

Kidney and hearts are other two target organs affected by SARS-CoV-2. Among hospitalized COVID-19 patients, the morbidity rate of acute kidney injury (AKI) was above 20 %, with higher mortality rate observed among individuals with preexisting diabetes mellitus (Diao et al., 2021; Puelles et al., 2020). Autopsy studies revealed cardiac (D'souza et al., 2017), diastolic dysfunction and heart failure in diabetic patients infected

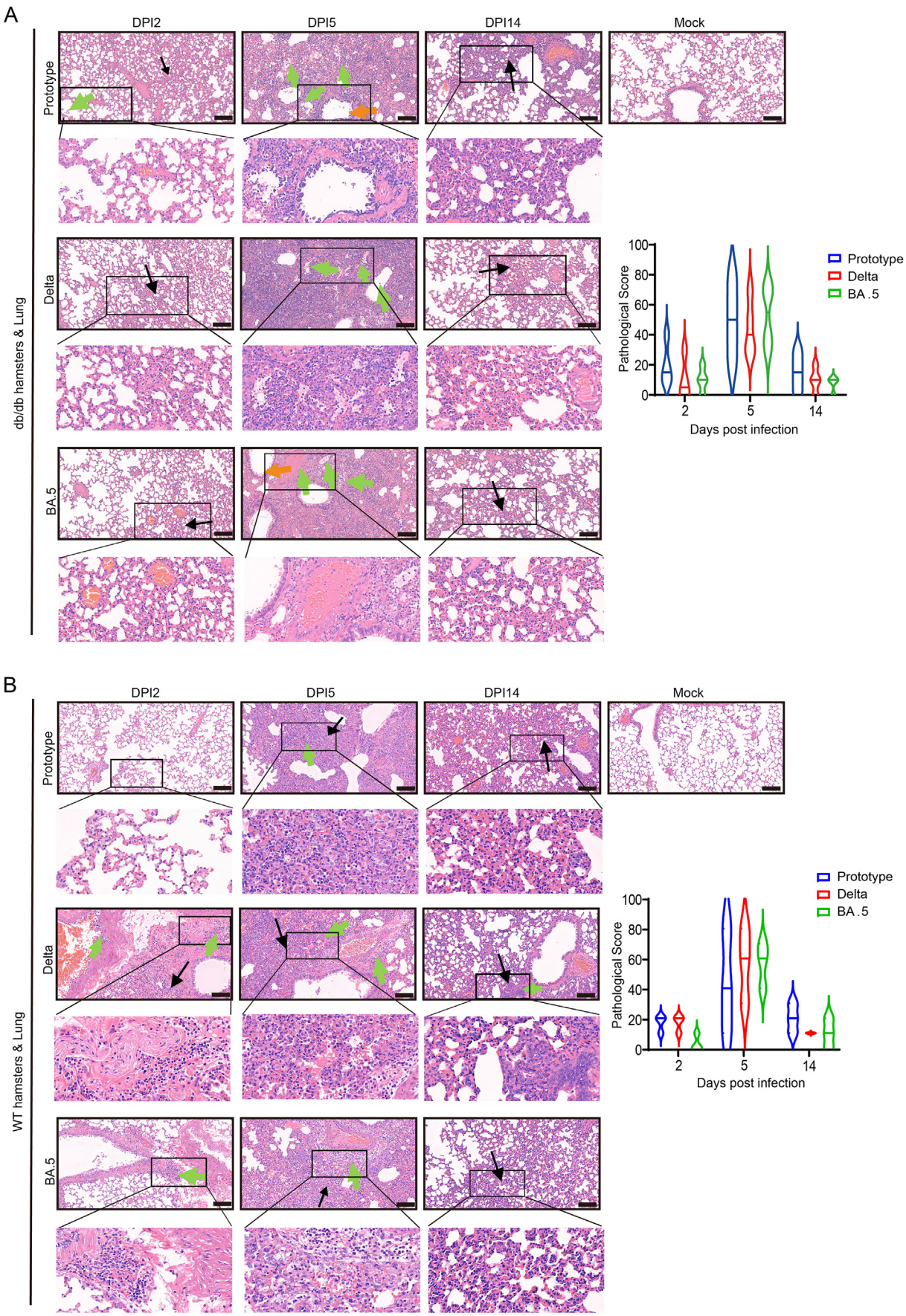

(caption on next page)

Fig. 4. The lung histopathological changes and pathological scoring in db/db hamsters and WT hamsters. **A, B** Six-to-ten-week-old male and female hamsters were mock-infected or intranasally infected with 1×10^5 $TCID_{50}$ of SARS-CoV-2 prototype, SARS-CoV-2 Delta variant, or SARS-CoV-2 Omicron BA.5 variant. Infected db/db hamsters (**A**) and WT hamsters (**B**) were sacrificed at 2, 5, and 14 DPI to examine the pathological changes in the lungs, while mock-infected hamsters were sacrificed at 14 DPI as the negative control group. Meanwhile, semiquantitative analysis and pathology scoring of the H&E-stained tissues section were performed. Images were collected using a Pannoramic MIDI system. In lung histopathology, black arrows indicate alveolar wall thickening and widening of the alveolar spacing; green arrows signify lymphocytic and granulocytic infiltration, and orange arrows denote bronchial epithelial cell necrosis. The scores were determined based on the percentage of inflammation in the pulmonary section by using the following 0–70 point scoring system: 0, no inflammation; 15, affected area (≤1 %); 30, affected area (>1 %, ≤10 %); 45, affected area (>10 %, ≤50 %); 60, affected area (>50 %). Additional 10 points were added when pulmonary edema, inflammatory cell infiltration, fibroplasia, and/or hyaline membrane formation were observed. The scale bar is 50 μm. Error bars indicate the standard error. Statistical significance was measured by two-way ANOVA. No significance was observed among different groups.

with SARS-CoV-2. Furthermore, it was reported that SARS-CoV-2 infection in obese mice exacerbated their chronic diseases such as cardiovascular diseases and diabetes. To investigate whether SARS-CoV-2 can intensify the diabetes-associated renal disease or it can cause severe pathological impairment of hearts in diabetic populations, we conducted H&E staining and analyzed the pathological features of kidneys and hearts in db/db hamsters and wild-type hamsters with SARS-CoV-2 variant infection.

In db/db hamsters from the mock group, minor kidney injury including a few scattered necrosis of renal tubular epithelial cells and cytoplasmic vacuolization (black arrows) was observed (Fig. 5A). In contrast, db/db hamsters infected with SARS-CoV-2 and variants developed more significant AKI at 5 DPI, and did not show signs of recovery by 14 DPI. The kidney histopathological characters were dilatation of glomerular capsules, enrichment of eosinophilic secretions (green arrows), atrophy of cortical medullary tubules (red arrows), necrosis of tubular epithelial cells, cytoplasmic vacuolization (black arrows), nuclear pyknosis, formation of a proteinaceous tubular pattern (yellow arrows), tubule dilatation with irregular lumens, flattening of tubular epithelial cells (orange arrows), and infiltration of lymphocytes (blue arrows). It is noteworthy that there was no significant difference between the pathology scoring of db/db hamster kidneys infected with different SARS-CoV-2 strains. The kidney pathological injury generated by Delta and Omicron BA.5 were not reduced in comparison with the prototype SARS-CoV-2. Besides, kidneys of infected wild-type hamsters displayed relatively mild lesions (Fig. 5B).

Regarding the histopathology of hearts, db/db hamsters exhibited varying degrees of lesions, characterized by mild to moderate hydropic degeneration of cardiomyocytes (black arrows) and breaks in myocardial fibers (red arrows) (Supplementary Fig. S1B). However, only very minor hydropic degeneration of cardiomyocytes was present in wild-type hamsters at 14 DPI (Supplementary Fig. S1C). Interestingly, the BA.5 variant, which was thought to have weakened virulence in human populations, led to heart injury equivalent to the prototype and Delta. These results were in consistence with what was observed in kidney.

Collectively, our comparative pathology of the two hamster models suggested that infection of SARS-CoV-2 and its variants caused more severe lung tissue injury in db/db hamsters than in wild-type hamsters. It

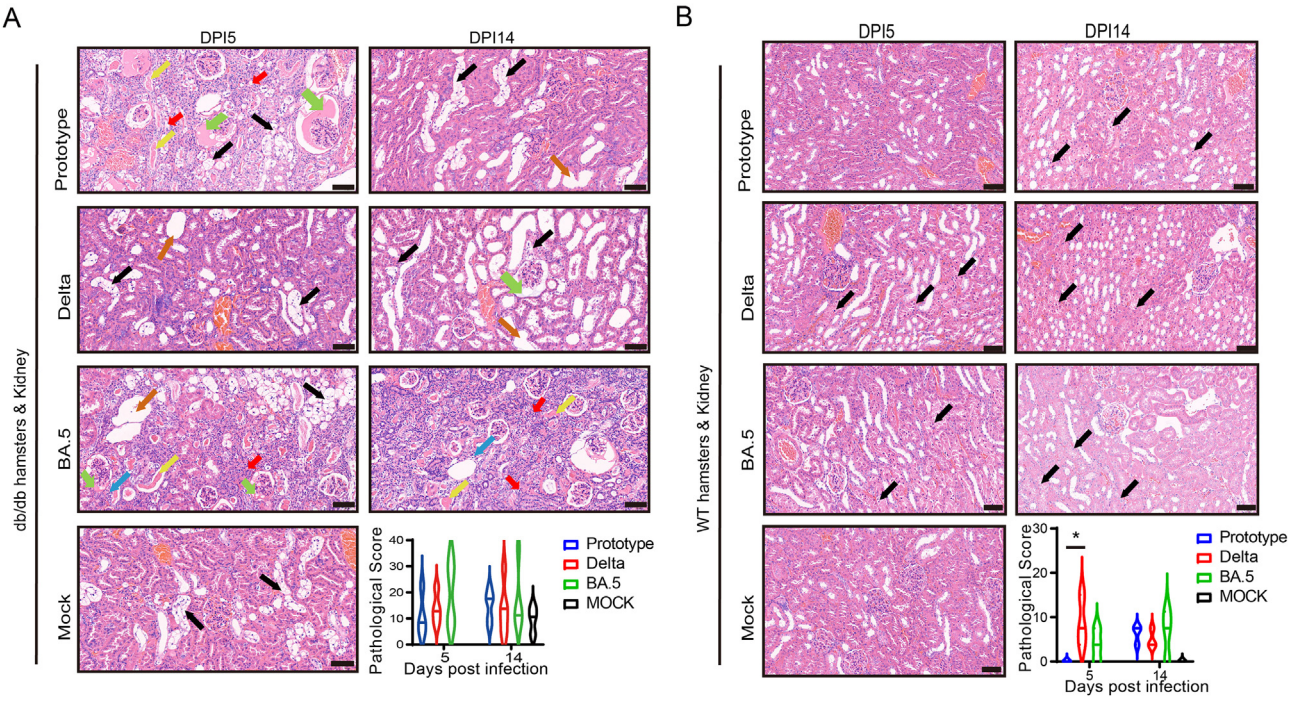

Fig. 5. The kidney histopathological changes and pathological scoring in db/db hamsters and WT hamsters. **A, B** Six-to-ten-week-old male and female hamsters were mock-infected or intranasally infected with 1×10^5 $TCID_{50}$ of SARS-CoV-2 prototype, SARS-CoV-2 Delta variant, or SARS-CoV-2 Omicron BA.5 variant. Infected db/db hamsters (**A**) and WT hamsters (**B**) were sacrificed at 2, 5, and 14 DPI to examine the pathological changes in the kidneys, while mock-infected hamsters were sacrificed at 14 DPI as the negative control group. Meanwhile, semiquantitative analysis and pathology scoring of the H&E-stained tissues section were conducted. Images were collected using a Pannoramic MIDI system. In kidney histopathology, black arrows represent necrosis of renal tubular epithelial cells and cytoplasmic vacuolization; green arrows indicate dilatation of the glomerular capsule filled with eosinophilic secretions; red arrows signify atrophy of cortical medullary tubules; yellow arrows indicate the formation of a proteinaceous tubular pattern; orange arrows denote tubule dilatation with irregular lumens and flattening of tubular epithelial cells, and blue arrows indicate lymphocyte infiltration. The scale bar is 50 μm. Error bars indicate the standard error. Statistical significance was measured by two-way ANOVA. * $P < 0.05$.

not only exacerbated the preexisting kidney injury in diabetic hamsters but also induced their cardiomyocytic lesions. Although the more recent variants of SARS-CoV-2 show reduced pathogenicity in lungs, we should remain vigilant about the potential risk they pose to other organs in patients with comorbidity of diabetes mellitus.

DISCUSSION

Diabetes mellitus is a global metabolic disease known as a risk factor for many emerging infectious diseases (Shah and Hux, 2003; Gao et al., 2020). For example, during the outbreaks or pandemics of SARS, H1N1 and MERS, the incidence rates of severe cases, hospitalized cases and mortality among diabetic patients were evidently higher than that in normal populations (Yang et al., 2006; Allard et al., 2010; Alraddadi et al., 2016). T2DM is the common type of diabetes, accounting for about 85%–90% of diabetic cases (http://www.diabetesatlas.org/). Previous clinical and epidemiological studies revealed that compared with non-diabetic cases, COVID-19 patients with preexisting T2DM were more likely to develop critical disease outcomes and had higher fatality risk (Barron et al., 2020; Wang et al., 2020; Singh and Khunti, 2022). The leptin receptor deficient mice are widely used as a standard animal model for T2DM researches. It was reported that db/db mice displayed increased morbidity after infection with mouse-adapted SARS-CoV-2 compared to the control group (Huang et al., 2023; Zhang et al., 2023). As a rodent model more susceptible to SARS-CoV-2 than mice, SARS-CoV-2-infecting golden hamsters exhibited lung pathological changes similar to that in humans, including bronchial epithelial cell necrosis, inflammatory cell infiltration, pulmonary ground glass opacity, body weight loss, and interstitial pneumonia or even death in individuals of severe infection (Chan et al., 2020; Sia et al., 2020). In the present study, we have constructed a T2DM hamster model by knockout of the leptin receptor gene. Persistently high respiratory virus load can be detected in our db/db hamster model after SARS-CoV-2 challenge. Meanwhile, this hamster model well replicated the clinical manifestation of diabetic patients infected with SARS-CoV-2 such as severe lung pathological injury, excessive pulmonary immune response, abnormality of blood biochemical indices, and more serious diabetes-associated complications (diabetic kidney disease and heart injury).

In addition to respiratory tracts, kidney is another important target organ of SARS-CoV-2 infection. AKI can occur in critical COVID-19 cases, especially in elderly patients and those with comorbidity of diabetes (Cheng et al., 2020; Puelles et al., 2020; Diao et al., 2021). Previous study reported that expression of the ACE2 receptor of SARS-CoV-2 in kidney was approximately 100-fold higher than that in lung tissue, and the risk of AKI induced by SARS-CoV-2 not only existed in diabetic patients but also in general populations (Cheng et al., 2020,Chen et al., 2020; Kronbichler et al., 2020). Diabetic kidney disease is a complication common in diabetic patients. As the renal vascular endothelial cells are affected by high concentration of blood glucose for long time, the cell morphology has been altered with basement membrane thickening and vasoconstriction, which results in decrease of reactivity of glomerular mesangial cells and renal cell dysfunction. In our db/db hamster model, long-term high blood glucose level has already led to mild pathological damage in its kidney. It developed pathological phenotypes of more severe AKI that resemble clinical cases after SARS-CoV-2 infection, including glomerular capsule dilatation, atrophy of cortical medullary tubules, tubular epithelial cell necrosis, tubule dilatation, tubular urine production, etc., suggesting that this model may well simulate the occurrence and progression of multiorgan diseases related to SARS-CoV-2 infection.

Several studies have preliminarily described the underlying mechanism for the increasing risk of severe COVID-19 in diabetic patients (Chen et al., 2023). Impaired capability of controlling blood glucose is a marked physiological feature of diabetes mellitus. Attention has been paid to investigating whether T2DM modulates the expression of key viral entry factors (such as ACE2 or TMPRSS2) essential for SARS-CoV-2 infectivity across various tissues. However, existing evidence remains inconclusive (Drucker, 2021). Some *in vitro* assays and *in vivo* studies in mouse models have demonstrated that overexpression of ACE can be stimulated by high blood glucose levels (Wysocki et al., 2006), probably due to the increased stability of ACE2 mRNA (Garreta et al., 2022), and elevated ACE2 expression can be responsible for promoting virus entry. It is thought that preexisting diabetes may facilitate the severity of COVID-19 partially via upregulating ACE2 expression and thus promote SARS-CoV-2 entry (Chen et al., 2023). However, our data demonstrate that diabetic hamsters do not exhibit significantly elevated lung ACE2 expression compared to wild-type hamsters (Supplementary Fig. S1D). Whether higher infectivity of SARS-CoV-2 in diabetic hamsters is associated with higher ACE2 expression cannot be determined. Regarding the mechanism of diabetes-related kidney injury exacerbation caused by SARS-CoV-2, it was previously found that SARS-CoV-2 N protein may induce severe AKI via Smad3-Ripk3/MLKL pathway, or through activation of Mincle-dependent M1 macrophages, in diabetic db/db mice (Liang et al., 2023; Wu et al., 2023). Other studies also suggested that kidney pathology by SARS-CoV-2 can be a consequence of both direct infection of target kidney cells and indirect lesions generated by immune response, circulatory dysfunction and hypoxia (Diao et al., 2021). As the diabetic hamster model constructed in this study can mimic the susceptibility, the lung inflammation response, as well as the multiorgan pathology of COVID-19 patients with diabetes, it may become a candidate model useful in further studies elucidating the disease mechanism of severe COVID-19 complicated with diabetes.

Diabetes mellitus is a systemic metabolic disorder characterized by chronic hyperglycemia, and it is associated with significant immune dysregulation that may impair viral clearance through multiple mechanisms. These include, but are not limited to, dysfunction in both innate and adaptive immune responses, altered cytokine profiles, and impaired leukocyte function. Previous clinical studies have demonstrated that virus infection (like H1N1) in obese patients is associated with prolonged viral shedding and extended periods of viral persistence (Maier et al., 2018). Also, multiple retrospective cohort studies have consistently demonstrated that SARS-CoV-2 infection in patients with T2DM is characterized by prolonged viral detection across multiple sites, including nasal and oropharyngeal swabs as well as bronchoalveolar lavage fluids (Buetti et al., 2020a, 2020b; Dicker et al., 2020). In our study, lower virus titers were detected in lung and turbinate of db/db hamsters compared with wild-type hamsters at 2 DPI but higher virus titers were detected in db/db hamsters at 5 DPI. This supports the findings of those previous clinical studies, in which there is a delay of virus detection and clearance in obese or diabetic patients. Metabolic disturbances in dendritic cells of the lungs of diabetic patients have been found to significantly reduce their antigen presentation and immune activation capacity, thereby increasing susceptibility to viral infections and delaying viral clearance (Nobs et al., 2023). Furthermore, a state of persistent hyperglycemia may inhibit the early clearance of viruses by macrophages and neutrophils, as well as the proliferation and activation of T-cells in fully adaptive immunity. This phenomenon has been further confirmed in mouse studies (Serreze et al., 2005; Toapanta and Ross, 2009; Oltolini et al., 2023). SARS-CoV-2 infection induces excessive release of inflammatory factors such as IL-6, TNF-α, and IL-1β, and this “inflammatory storm” leads to viral-associated tissue damage (Wang et al., 2020); however, persistent hyperglycemia further contributes to the dysregulation of inflammatory factors, exacerbating the damage to organs caused by the inflammatory storm (Singh and Khunti, 2022). Such hyperglycemia-associated immune dysregulation may explain the enhanced proinflammatory responses and more severe outcomes observed in the diabetic hamsters in this study.

With the large-scale and long-term prevalence and infection among global populations, SARS-CoV-2 is keeping on evolving and mutating. Novel variants of SARS-CoV-2 has been continuously born, replacing the previously existing variants and becoming new predominant strains. Evidence have shown increased transmissibility of the more recently emerging SARS-CoV-2 variants, represented by the different sub-lineages

of Omicron variants, but their respiratory pathogenicity seems to have declined (Chan et al., 2022; Shuai et al., 2022, 2023; Hu et al., 2024). In our db/db hamster model with SARS-CoV-2 infection, both the virus load testing and lung histopathology results suggested that the pathogenicity of the variants were attenuated compared to the prototype strain, whereas we still need to be cautious that the injury in other tissues like kidney and heart caused by SARS-CoV-2 variants remains in the db/db hamsters, and that SARS-CoV-2 and the variants can trigger stronger proinflammatory cytokine and chemokine storm (IL-4, IL-10, CXCL9, CXCL10, CCL5, and IL-1β) in lungs of db/db hamsters than in wild-type hamsters. Previous studies revealed a bidirectional relationship of diabetes and COVID-19. Diabetes can promote the fatality rate of COVID-19 and reduce the protective efficacy of SARS-CoV-2 vaccines (Johnson et al., 2023). On the other hand, infection of SARS-CoV-2 including the Omicron variants may increase the risk of diabetes occurrence, which is in consistence with the elevated blood glucose level that we observed in SARS-CoV-2-infecting wild-type hamsters (Xie and Al-Aly, 2022; Kwan et al., 2023). Additionally, since elderly people are high-risk populations for both diabetes and COVID-19, the double factors, aging in combination with diabetes, further augment the risk of severe COVID-19 among these susceptible populations. In summary, despite the relatively lower virulence of currently circulating SARS-CoV-2 variants, the potential public health hazard they pose especially to those with diabetes should never the underestimated, as repeated breaking SARS-CoV-2 infection can result in an increasing number of diabetic patients and cause multiorgan comorbidities, thus aggravating disease burden of the public.

CONCLUSIONS

In summary, we have established an animal infection model of SARS-CoV-2 and its variants using golden hamsters with T2DM. This model developed severe multiorgan injury and strong inflammation response after being infected with SARS-CoV-2 and variants, and it recapitulated the acute and severe pathological process of COVID-19 complicated with diabetes. It suggests lasting risk of the evolving SARS-CoV-2 variants to the health of diabetic patients. Our diabetic hamster model offers a tool that may help better understand the pathogenesis mechanism of severe SARS-CoV-2 infection in people with diabetes, and will aid in screening and testing antivirals, vaccines or other countermeasures against SARS-CoV-2 variants or even other sarbecoviruses among these high-risk populations.

MATERIALS AND METHODS

Viruses and cells

Viruses of SARS-CoV-2 strains were acquired from the National Virus Resource Center. All virus-related work was conducted within a Biosafety Level 3 (BSL-3) containment facility. All viruses were propagated and titrated in *Cercopithecus aethiops* kidney cells (Vero E6, ATCC® CRL-1586). Vero E6 cells were cultured in DMEM (Gibco, USA) supplemented with 10 % fetal bovine serum (FBS, Gibco) and 1% Anti-Anti (Invitrogen, USA) at 37 °C in the presence of 5% CO_2.

Generation of leptin receptor-deficient (db/db) hamsters

Golden hamsters were sourced from Charles River Laboratories (Beijing, China) and housed under a 14-h light/10-h dark cycle in the Nanjing Medical University animal facility. All experimental protocols were approved by the Animal Care and Use Committee of Nanjing Medical University.

Single-guide RNAs (sgRNAs) were designed using CRISPRdirect (http://crispr.dbcls.jp/) and CRISPOR (http://crispor.tefor.net/). Complementary target oligonucleotides were inserted into the pUC57-T7-sgRNA-trcRNA vector at the *Bsa*I restriction site. PCR amplification was used to generate templates containing the T7 promoter and sgRNA sequences for *in vitro* transcription with the HiScribe T7 High Yield RNA Synthesis Kit (NEB, E2040S). Purified sgRNAs were stored at −80 °C following lithium chloride precipitation.

To generate genome-edited golden hamsters, we injected CRISPR-Cas9 protein (IDT) and sgRNA into two-cell embryos under a red-filtered microscope. Cultured in mHECM9+HSA medium under a humidified 10% CO_2 environment at 37.5 °C for 15–30 min, the embryos were then transferred into the oviducts of 0.5-day pregnant recipients, with 15–30 embryos per recipient. Founder pups were mated with wild-type counterparts to produce the F1 generation, and genotyping was conducted using the one-step mouse genotyping kit as per manufacturer's protocol (Vazyme, PD101-01).

Genotyping of db/db hamsters

Genotyping of db/db golden hamsters was conducted using the one-step mouse genotyping kit in accordance with the manufacturer's instructions (Vazyme, PD101-01). Genomic DNA was extracted from hamster tails, which were lysed by incubation in 50 μL of lysis buffer (100 mM Tris-HCl, pH 8, 5 mM EDTA, 0.2% SDS, 200 mM NaCl) with 1 μL of 20 mg/mL Proteinase K. Samples were shaken at 55 °C for 15 min, followed by centrifugation at 10,000 ×*g* for 5 min. The supernatant was transferred to a new Eppendorf tube to obtain the DNA. All hamsters were genotyped by genomic PCR as previously described.

Western blot analysis

Subcutaneous inguinal adipose tissues for Western blot were obtained from wild-type or db/db hamsters. Total proteins were extracted in 95% Laemmle sample buffer, separated on 10% SDS-PAGE using the Mini-PROTEAN Tetra Cell System (Bio-Rad), and electrophoretically transferred to polyvinylidene difluoride membranes. Anti-GAPDH mouse monoclonal antibodies (Proteintech, 1:10,000) and anti-Leptein receptor rabbit polyclonal antibodies (HUABIO, 1:2000) were used as primary antibodies and incubated with the membranes at 4 °C for 12 h. After washing twice with PBS containing 0.2% Tween-20 (PBST), the membranes were incubated with HRP-linked goat anti-rabbit antibodies (ThermoFisher Scientific, 31,466, 1:5000) or HRP-linked anti-mouse IgG (ThermoFisher Scientific, 31,430, 1:5000) at room temperature for 1 h before visualization using the ECL Detection kit (GE Healthcare).

Animal infection experiments

Six-to-ten-week-old wild-type hamsters and db/db hamsters were inoculated with 1×10^5 $TCID_{50}$ of SARS-CoV-2 (prototype, Delta, or Omicron BA.5 strains). Additionally, hamsters were mock-infected with the same volume of DMEM as controls. For survival monitoring, the SARS-CoV-2-infected wild-type and db/db hamsters (2 males and 3 females for each strain) and mock-infected hamsters (1 male and 2 females) were monitored for 14 days. For tissue collection, the infected wild-type (5 males and 4 females for each strain, with 3 animals including both males and females randomly selected at each indicated time point) and db/db hamsters (6 males and 7 females for each strain, with 4 or 5 animals including both males and females randomly selected at each indicated time point) were euthanized for tissue collection. Hamsters were virus-inoculated under proper anesthesia, and efforts were made to minimize any potential pain and distress. Clinical manifestations and survival were recorded for 14 days. Heart, lung, kidney and subcutaneous inguinal adipose were harvested.

Determination of virus titers in tissues

Vero E6 cells were seeded in 24-well plates one day before use. Infected tissues were homogenized in DMEM. The cells were inoculated

with tissue dilutions for 1 h. Next, the inoculum was removed, and the cells were incubated with 0.9% methylcellulose for 5 days. Plaque-forming units (PFU) were counted after crystal violet staining to calculate the viral titer.

RNA extraction and RT-qPCR

The lung of WT hamsters and db/db hamsters were collected and homogenized in Vezol Reagent, and RNA was extracted using the VeZol-Pure Total RNA Isolation Kit (RC202, Vazyme, China). *ACE2* gene and *GAPDH* gene was detected using the HiScript II One Step qRT-PCR SYBR Green Kit (Applied Biosystems, USA) and the following specific primers: ACE2 (Forward: 5′-TCCATTGGTCTTCTGCCATCCG-3′, Reverse: 5′-AGACCATCCACCTCCACTTCTC-3′) and GAPDH (Forward: 5′-CTGAGACACAATGGTGAAGGTCG′, Reverse: 5′-CGTTCTCAGCCTTGACTGTGC-3′). The relative gene expression level of ACE2 was quantified using the ΔΔCt method, normalized to the endogenous reference gene GAPDH in the host.

Cytokine detection

Total RNA was extracted from lung lysates using a FastPure Cell/Tissue Total RNA Isolation Kit (Vazyme, China) according to a manufacturer's instructions. RNA was detected using the HiScript® II One-Step qRT-PCR SYBR® Green Kit (Applied Biosystems, USA) with different specific primers. Primer sequences is presented in the Supplementary Table S1. Gene expression fold-changes were calculated using the $2^{-\Delta\Delta Ct}$ method in Microsoft Excel.

Blood sampling and biochemistry

Plasma was separated by centrifugation at 3000×*g* for 10 min at room temperature and stored at −80 °C until use. 40 μL plasma was collected and the biochemistry (BUN, ALT, CHOL LIPA, TP, CK, and LDH) were tested using Catalyst One (IDEXX) followed with manufacturer's instructions.

Histological analysis

Organ samples were collected in formalin and embedded in paraffin for pathological analysis. Fixed samples were used for H&E staining, which were conducted using optimized assays, as previously described (Jiang et al., 2020). Meanwhile, Scoring of pathology in H&E-stained tissue sections were performed following internationally recognized standards, with adjustments made to accommodate the unique characteristics of the tissue sections (Mann, 2019; Lin et al., 2023).

Statistical analysis

All data were analyzed using one-way ANOVA or two-way ANOVA (GraphPad). Results are presented as the means ± SEM. $P < 0.05$ is considered significant (significance is denoted as follows: ns, no significance; $*P \leq 0.05$; $**P \leq 0.01$; $***P \leq 0.001$).

DATA AVAILABILITY

All data supporting the conclusions of this study are reported in the paper. The raw data are available from the corresponding author with no restrictions upon reasonable request.

ETHICS STATEMENT

All animal infection experiments were approved by the institutional Animal Care and Use Committee (approval number: WIVA05202201).

AUTHOR CONTRIBUTIONS

Hao-Feng Lin: date curation, formal analysis, investigation, methodology, software, validation, visualization, writing-original draft, writing-review & editing. Ren-Di Jiang: investigation, methodology, validation, writing-review & editing. Rui-Xin Qin: formal analysis, investigation, resources. Bing Yao: methodology, resources. Wen-Tao Zeng: investigation, resources. Yun-Gao: investigation, methodology, resources. Ai-Min Shi: conceptualization, funding acquisition, methodology, resources, supervision. Jian-Min Li: conceptualization, funding acquisition, project administration, resources, supervision, visualization, writing-review & editing. Mei-Qin Liu: data curation, formal analysis, investigation, methodology, validation, writing-review & editing. All authors have read and agreed to the version of the manuscript.

CONFLICT OF INTEREST

All authors declare that there are no competing interests.

ACKNOWLEDGMENTS

We thank Dr. Tao Du, Mr. Jin Xiong, and Ms. Min Hou from the National Biosafety Laboratory, Wuhan, for their essential support. We thank Ms. Jing Deng and Dr. Yanfeng Yao for animal care and management. We thank Zi-Shuo Guo for his assistance in animal infection experiments. We thank Dr. Ben Hu for his significant contribution in this study. This work was jointly supported by the National Natural Science Foundation of Jiangsu Province (BE20197310 to J-M.L.), the National Key R&D Program of China (2021YFF0702500 to J-M.L. and A-M.S., and the Start-up Funding of Scientific Researches for Postdoc in Guangzhou, Guangdong Province to H–F.L.).

APPENDIX A. SUPPLEMENTARY DATA

Supplementary data to this article can be found online at https://doi.org/10.1016/j.virs.2025.05.001.

REFERENCES

Allard, R., Leclerc, P., Tremblay, C., Tannenbaum, T.N., 2010. Diabetes and the severity of pandemic influenza A (H1N1) infection. Diabetes Care 33, 1491–1493.

Alraddadi, B.M., Watson, J.T., Almarashi, A., Abedi, G.R., Turkistani, A., Sadran, M., Housa, A., Almazroa, M.A., Alraihan, N., Banjar, A., Albalawi, E., Alhindi, H., Choudhry, A.J., Meiman, J.G., Paczkowski, M., Curns, A., Mounts, A., Feikin, D.R., Marano, N., Swerdlow, D.L., Gerber, S.I., Hajjeh, R., Madani, T.A., 2016. Risk factors for primary Middle East respiratory syndrome coronavirus illness in humans, Saudi arabia, 2014. Emerg. Infect. Dis. 22, 49–55.

Barron, E., Bakhai, C., Kar, P., Weaver, A., Bradley, D., Ismail, H., Knighton, P., Holman, N., Khunti, K., Sattar, N., Wareham, N.J., Young, B., Valabhji, J., 2020. Associations of type 1 and type 2 diabetes with COVID-19-related mortality in England: a whole-population study. Lancet Diabetes Endocrinol 8, 813–822.

Buetti, N., Trimboli, P., Mazzuchelli, T., Lo Priore, E., Balmelli, C., Trkola, A., Conti, M., Martinetti, G., Elzi, L., Ceschi, A., Consonni, V., Ogna, A., Forni-Ogna, V., Bernasconi, E., 2020a. Diabetes mellitus is a risk factor for prolonged SARS-CoV-2 viral shedding in lower respiratory tract samples of critically ill patients. Endocrine 70, 454–460.

Buetti, N., Wicky, P.H., Le Hingrat, Q., Ruckly, S., Mazzuchelli, T., Loiodice, A., Trimboli, P., Forni Ogna, V., De Montmollin, E., Bernasconi, E., Visseaux, B., Timsit, J.F., 2020b. SARS-CoV-2 detection in the lower respiratory tract of invasively ventilated ARDS patients. Crit. Care 24, 610.

Cao, Y., Jian, F., Wang, J., Yu, Y., Song, W., Yisimayi, A., Wang, J., An, R., Chen, X., Zhang, N., Wang, Y., Wang, P., Zhao, L., Sun, H., Yu, L., Yang, S., Niu, X., Xiao, T., Gu, Q., Shao, F., Hao, X., Xu, Y., Jin, R., Shen, Z., Wang, Y., Xie, X.S., 2023. Imprinted SARS-CoV-2 humoral immunity induces convergent Omicron RBD evolution. Nature 614, 521–529.

Carabelli, A.M., Peacock, T.P., Thorne, L.G., Harvey, W.T., Hughes, J., Consortium, C.-G.U., Peacock, S.J., Barclay, W.S., De Silva, T.I., Towers, G.J., Robertson, D.L., 2023. SARS-CoV-2 variant biology: immune escape, transmission and fitness. Nat. Rev. Microbiol. 21, 162–177.

Chan, J.F.W., Yuan, S.F., Zhang, A.J.X., Poon, V.K.M., Chan, C.C.S., Lee, A.C.Y., Fan, Z.M., Li, C., Liang, R.H., Cao, J.L., Tang, K., Luo, C., Cheng, V.C., Cai, J.P., Chu, H., Chan, K.H., To, K.K., Sridhar, S., Yuen, K.Y., 2020. Surgical mask partition reduces the risk of noncontact transmission in a golden Syrian hamster model for coronavirus disease 2019 (COVID-19). Clin. Infect. Dis. 71, 2139–2149.

Chan, J.F., Hu, B., Chai, Y., Shuai, H., Liu, H., Shi, J., Liu, Y., Yoon, C., Zhang, J., Hu, J.C., Hou, Y., Huang, X., Yuen, T.T., Zhu, T., Li, W., Cai, J.P., Luo, C., Yip, C.C., Zhang, A.J., Zhou, J., Yuan, S., Zhang, B.Z., Huang, J.D., To, K.K., Yuen, K.Y., Chu, H., 2022. Virological features and pathogenicity of SARS-CoV-2 Omicron BA.2. Cell Rep. Med. 3, 100743.

Chen, H., Charlat, O., Tartaglia, L.A., Woolf, E.A., Weng, X., Ellis, S.J., Lakey, N.D., Culpepper, J., Moore, K.J., Breitbart, R.E., Duyk, G.M., Tepper, R.I., Morgenstern, J.P., 1996. Evidence that the diabetes gene encodes the leptin receptor: identification of a mutation in the leptin receptor gene in db/db mice. Cell 84, 491–495.

Chen, N.S., Zhou, M., Dong, X., Qu, J.M., Gong, F.Y., Han, Y., Qiu, Y., Wang, J.L., Liu, Y., Wei, Y., Xia, J., Yu, T., Zhang, X., Zhang, L., 2020. Epidemiological and clinical characteristics of 99 cases of 2019 novel coronavirus pneumonia in Wuhan, China: a descriptive study. Lancet 395, 507–513.

Chen, T., Wu, D., Chen, H., Yan, W., Yang, D., Chen, G., Ma, K., Xu, D., Yu, H., Wang, H., Wang, T., Guo, W., Chen, J., Ding, C., Zhang, X., Huang, J., Han, M., Li, S., Luo, X., Zhao, J., Ning, Q., 2020b. Clinical characteristics of 113 deceased patients with coronavirus disease 2019: retrospective study. BMJ 368, m1091.

Chen, P., Wu, M., He, Y., Jiang, B., He, M.L., 2023. Metabolic alterations upon SARS-CoV-2 infection and potential therapeutic targets against coronavirus infection. Signal Transduct. Targeted Ther. 8, 237.

Cheng, Y., Luo, R., Wang, K., Zhang, M., Wang, Z., Dong, L., Li, J., Yao, Y., Ge, S., Xu, G., 2020. Kidney disease is associated with in-hospital death of patients with COVID-19. Kidney Int. 97, 829–838.

Coronaviridae Study Group of the International Committee on Taxonomy Of Virus, 2020. The species Severe acute respiratory syndrome-related coronavirus: classifying 2019-nCoV and naming it SARS-CoV-2. Nat. Microbiol. 5, 536–544.

D'souza, A.,M., Neumann, U.H., Glavas, M.M., Kieffer, T.J., 2017. The glucoregulatory actions of leptin. Mol. Metabol. 6, 1052–1065.

Davies, N.G., Abbott, S., Barnard, R.C., Jarvis, C.I., Kucharski, A.J., Munday, J.D., Pearson, C.a.B., Russell, T.W., Tully, D.C., Washburne, A.D., Wenseleers, T., Gimma, A., Waites, W., Wong, K.L.M., van Zandvoort, K., CMMID COVID-19 Working Group, COVID-19 Genomics UK (COG-UK) Consortium, Silverman, J.D., Diaz-Ordaz, K., Keogh, R., Eggo, R.M., Funk, S., Jit, M., Atkins, K.E., Edmunds, W.J., 2021a. Estimated transmissibility and impact of SARS-CoV-2 lineage B.1.1.7 in England. Science 372, 6538.

Davies, N.G., Jarvis, C.I., Group, C.C.-W., Edmunds, W.J., Jewell, N.P., Diaz-Ordaz, K., Keogh, R.H., 2021b. Increased mortality in community-tested cases of SARS-CoV-2 lineage B.1.1.7. Nature 593, 270–274.

Diao, B., Wang, C., Wang, R., Feng, Z., Zhang, J., Yang, H., Tan, Y., Wang, H., Wang, C., Liu, L., Liu, Y., Liu, Y., Wang, G., Yuan, Z., Hou, X., Ren, L., Wu, Y., Chen, Y., 2021. Human kidney is a target for novel severe acute respiratory syndrome coronavirus 2 infection. Nat. Commun. 12, 2506.

Dicker, D., Lev, S., Gottesman, T., Kournos, T., Dotan, M., Ashorov, N., Marcoviciu, D., Golan, R., 2020. A time frame for testing negative for SARS-COV2 in people with obesity. Obes. Facts 13, 528–533.

Drucker, D.J., 2021. Diabetes, obesity, metabolism, and SARS-CoV-2 infection: the end of the beginning. Cell Metab. 33, 479–498.

Faria, N.R., Mellan, T.A., Whittaker, C., Claro, I.M., Candido, D.D.S., Mishra, S., Crispim, M.a.E., Sales, F.C.S., Hawryluk, I., Mccrone, J.T., et al., 2021. Genomics and epidemiology of the P.1 SARS-CoV-2 lineage in Manaus, Brazil. Science 372, 815–821.

Gao, Y.D., Ding, M., Dong, X., Zhang, J.J., Kursat Azkur, A., Azkur, D., Gan, H., Sun, Y.L., Fu, W., Li, W., Liang, H.L., Cao, Y.Y., Yan, Q., Cao, C., Gao, H.Y., Brüggen, M.C., van de Veen, W., Sokolowska, M., Akdis, M., Akdis, C.A., 2020. Risk factors for severe and critically ill COVID-19 patients: a review. Allergy 76, 428–455.

Garreta,, E., Prado,, P., Stanifer,, M.L., Monteil,, V., Marco,, A., Ullate-Agote,, A., Moya-Rull,, D., Vilas-Zornoza,, A., Tarantino,, C., Romero,, J.P., Jonsson, G., Oria, R., Leopoldi, A., Hagelkruys, A., Gallo, M., González, F., Domingo-Pedrol, P., Gavaldà, A., Del Pozo, C.H., HasanAli, O., Ventura-Aguiar, P., Campistol, J.M., Prosper, F., Mirazimi, A., Boulant, S., Penninger, J.M., Montserrat, N., 2022. A diabetic milieu increases ACE2 expression and cellular susceptibility to SARS-CoV-2 infections in human kidney organoids and patient cells. Cell Metab 34, 857–873.e9.

Gogiraju, R., Witzler, C., Shahneh, F., Hubert, A., Renner, L., Bochenek, M.L., Zifkos, K., Becker, C., Thati, M., Schafer, K., 2023. Deletion of endothelial leptin receptors in mice promotes diet-induced obesity. Sci. Rep. 13, 8276.

Gu, H.J., Chen, Q., Yang, G., He, L., Fan, H., Deng, Y.Q., Wang, Y.X., Teng, Y., Zhao, Z.P., Cui, Y.J., Li, Y., Li, X.F., Li, J., Zhang, N.N., Yang, X., Chen, S., Guo, Y., Zhao, G., Wang, X., Luo, D.Y., Wang, H., Yang, X., Li, Y., Han, G., He, Y., Zhou, X., Geng, S., Sheng, X., Jiang, S., Sun, S., Qin, C.F., Zhou, Y., 2020. Adaptation of SARS-CoV-2 in BALB/c mice for testing vaccine efficacy. Science 369, 1603–1607.

Hachmann, N.P., Miller, J., Collier, A.Y., Ventura, J.D., Yu, J., Rowe, M., Bondzie, E.A., Powers, O., Surve, N., Hall, K., Barouch, D.H., 2022. Neutralization escape by SARS-CoV-2 Omicron subvariants BA.2.12.1, BA.4, and BA.5. N. Engl. J. Med. 387, 86–88.

Halfmann, P.J., Iida, S., Iwatsuki-Horimoto, K., Maemura, T., Kiso, M., Scheaffer, S.M., Darling, T.L., Joshi, A., Loeber, S., Singh, G., et al., 2022. SARS-CoV-2 Omicron virus causes attenuated disease in mice and hamsters. Nature 603, 687–692.

Hu, B., Chan, J.F., Liu, Y., Liu, H., Chen, Y.X., Shuai, H., Hu, Y.F., Hartnoll, M., Chen, L., Xia, Y., Hu, J.C., Yuen, T.T., Yoon, C., Hou, Y., Huang, X., Chai, Y., Zhu, T., Shi, J., Wang, Y., He, Y., Cai, J.P., Zhou, J., Yuan, S., Zhang, J., Huang, J.D., Yuen, K.Y., To, K.K., Zhang, B.Z., Chu, H., 2024. Divergent trajectory of replication and intrinsic pathogenicity of SARS-CoV-2 Omicron post-BA.2/5 subvariants in the upper and lower respiratory tract. EBioMedicine 99, 104916.

Huang, C., Wang, Y., Li, X., Ren, L., Zhao, J., Hu, Y., Zhang, L., Fan, G., Xu, J., Gu, X., Cheng, Z., Yu, T., Xia, J., Wei, Y., Wu, W., Xie, X., Yin, W., Li, H., Liu, M., Xiao, Y., Gao, H., Guo, L., Xie, J., Wang, G., Jiang, R., Gao, Z., Jin, Q., Wang, J., Cao, B., 2020. Clinical features of patients infected with 2019 novel coronavirus in Wuhan, China. Lancet 395, 497–506.

Huang, K., Zhang, Y.F., Hui, X.F., Zhao, Y., Gong, W.X., Wang, T., Zhang, S.R., Yang, Y., Deng, F., Zhang, Q., Chen, X., Yang, Y., Sun, X., Chen, H., Tao, Y.J., Zou, Z., Jin, M., 2021. Q493K and Q498H substitutions in Spike promote adaptation of SARS-CoV-2 in mice. EBioMedicine 67, 103381.

Huang, Q., An, R., Wang, H., Yang, Y., Tang, C., Wang, J., Yu, W., Zhou, Y., Zhang, Y., Wu, D., Li, B., Yang, H., Lu, S., Peng, X., 2023. Aggravated pneumonia and diabetes in SARS-CoV-2 infected diabetic mice. Emerg. Microb. Infect. 12, 2203782.

Imai, M., Iwatsuki-Horimoto, K., Hatta, M., Loeber, S., Halfmann, P.J., Nakajima, N., Watanabe, T., Ujie, M., Takahashi, K., Ito, M., Yamada, S., Fan, S., Chiba, S., Kuroda, M., Guan, L., Takada, K., Armbrust, T., Balogh, A., Furusawa, Y., Okuda, M., Ueki, H., Yasuhara, A., Sakai-Tagawa, Y., Lopes, T.J.S., Kiso, M., Yamayoshi, S., Kinoshita, N., Ohmagari, N., Hattori, S.I., Takeda, M., Mitsuya, H., Krammer, F., Suzuki, T., Kawaoka, Y., 2020. Syrian hamsters as a small animal model for SARS-CoV-2 infection and countermeasure development. Proc. Natl. Acad. Sci. U. S. A. 117, 16587–16595.

Jiang, R.D., Liu, M.Q., Chen, Y., Shan, C., Zhou, Y.W., Shen, X.R., Q., Li., Zhang, L., Zhu, Y., Si, H.R., Wang, Q., Min, J., Wang, X., Zhang, W., Li, B., Zhang, H.J., Baric, R.S., Zhou, P., Yang, X.L., Shi, Z.L., 2020. Pathogenesis of SARS-CoV-2 in transgenic mice expressing human angiotensin-converting enzyme 2. Cell 182, 50–58.e8.

Johnson, R.M., Ardanuy, J., Hammond, H., Logue, J., Jackson, L., Baracco, L., Mcgrath, M., Dillen, C., Patel, N., Smith, G., Frieman, M., 2023. Diet-induced obesity and diabetes enhance mortality and reduce vaccine efficacy for SARS-CoV-2. J. Virol. 97, e0133623.

Kronbichler, A., Gauckler, P., Windpessl, M., Il Shin, J., Jha, V., Rovin, B.H., Oberbauer, R., 2020. COVID-19: implications for immunosuppression in kidney disease and transplantation. Nat. Rev. Nephrol. 16, 365–367.

Kwan, A.C., Ebinger, J.E., Botting, P., Navarrette, J., Claggett, B., Cheng, S., 2023. Association of COVID-19 vaccination with risk for incident diabetes after COVID-19 infection. JAMA Netw. Open 6, e2255965.

Li, B., Deng, A., Li, K., Hu, Y., Li, Z., Shi, Y., Xiong, Q., Liu, Z., Guo, Q., Zou, L., et al., 2022. Viral infection and transmission in a large, well-traced outbreak caused by the SARS-CoV-2 Delta variant. Nat. Commun. 13, 460.

Li, P., Faraone, J.N., Hsu, C.C., Chamblee, M., Liu, Y., Zheng, Y.M., Xu, Y., Carlin, C., Horowitz, J.C., Mallampalli, R.K., et al., 2024. Neutralization and stability of JN.1-derived LB.1, KP.2.3, KP.3 and KP.3.1.1 subvariants. bioRxiv. https://doi.org/10.1101/2024.09.04.611219.

Liang, L., Wang, W., Chen, J., Wu, W., Huang, X.R., Wei, B., Zhong, Y., Ma, R.C.W., Yu, X., Lan, H.Y., 2023. SARS-CoV-2 N protein induces acute kidney injury in diabetic mice via the Smad3-Ripk3/MLKL necroptosis pathway. Signal Transduct. Targeted Ther. 8, 147.

Lin, H.F., Liu, M.Q., Jiang, R.D., Gong, Q.C., Su, J., Guo, Z.S., Chen, Y., Jia, J.K., Dong, T.Y., Zhu, Y., Li, A., Shen, X.R., Wang, Y., Li, B., Xie, T.T., Yang, X.L., Hu, B., Shi, Z.L., 2023. Characterization of a mouse-adapted strain of bat severe acute respiratory syndrome-related coronavirus. J. Virol. 97, e0079023.

Liu, Y., Rocklov, J., 2022. The effective reproductive number of the Omicron variant of SARS-CoV-2 is several times relative to Delta. J. Trav. Med. 29, taac037.

Liu, J., Li, S., Liu, J., Liang, B., Wang, X., Wang, H., Li, W., Tong, Q., Yi, J., Zhao, L., Xiong, L., Guo, C., Tian, J., Luo, J., Yao, J., Pang, R., Shen, H., Peng, C., Liu, T., Zhang, Q., Wu, J., Xu, L., Lu, S., Wang, B., Weng, Z., Han, C., Zhu, H., Zhou, R., Zhou, H., Chen, X., Ye, P., Zhu, B., Wang, L., Zhou, W., He, S., He, Y., Jie, S., Wei, P., Zhang, J., Lu, Y., Wang, W., Zhang, L., Li, L., Zhou, F., Wang, J., Dittmer, U., Lu, M., Hu, Y., Yang, D., Zheng, X., 2020. Longitudinal characteristics of lymphocyte responses and cytokine profiles in the peripheral blood of SARS-CoV-2 infected patients. EBioMedicine 55, 102763.

Looi, M.K., 2023. Covid-19: WHO adds JN.1 as new variant of interest. BMJ 383, 2975.

Maier, H.E., Lopez, R., Sanchez, N., Ng, S., Gresh, L., Ojeda, S., Burger-Calderon, R., Kuan, G., Harris, E., Balmaseda, A., Gordon, A., 2018. Obesity increases the duration of influenza A virus shedding in adults. J. Infect. Dis. 218, 1378–1382.

Mann, P.C., 2019. 大鼠和小鼠病理变化术语及诊断标准的国际规范 (INHAND). 中国农业出版社,中国.

Mao, Y., Chen, Y., Li, Y., Ma, L., Wang, X., Wang, Q., He, A., Liu, X., Dong, T., Gao, W., Xu, Y., Liu, L., Ren, L., Liu, Q., Zhou, P., Hu, B., Zhou, Y., Tian, R., Shi, Z.L., 2024. Deep spatial proteomics reveals region-specific features of severe COVID-19-related pulmonary injury. Cell Rep 43, 113689.

Nobs, S.P., Kolodziejczyk, A.A., Adler, L., Horesh, N., Botscharnikow, C., Herzog, E., Mohapatra, G., Hejndorf, S., Hodgetts, R.J., Spivak, I., Schorr, L., Fluhr, L., Kviatcovsky, D., Zacharia, A., Njuki, S., Barasch, D., Stettner, N., Dori-Bachash, M., Harmelin, A., Brandis, A., Mehlman, T., Erez, A., He, Y., Ferrini, S., Puschhof, J., Shapiro, H., Kopf, M., Moussaieff, A., Abdeen, S.K., Elinav, E., 2023. Lung dendritic-cell metabolism underlies susceptibility to viral infection in diabetes. Nature 624, 645–652.

Oliveira, S., Monteiro-Alfredo, T., Henriques, R., Ribeiro, C.F., Seica, R., Cruz, T., Cabral, C., Fernandes, R., Piedade, F., Robalo, M.P., Matafome, P., Silva, S., 2022. Improvement of glycaemia and endothelial function by a new low-dose curcuminoid in an animal model of type 2 diabetes. Int. J. Mol. Sci. 23, 5652.

Oltolini, C., Acerbis, A., Orofino, G., Racca, S., Noviello, M., Dispinseri, S., Clementi, N., Piemontese, S., Xue, E., Giglio, F., Lupo Stanghellini, M.T., Diral, E., Bruno, A., Tassi, E., Beretta, V., Marzinotto, I., Scarlatti, G., Lampasona, V., Ardemagni, A., Sampaolo, M., Bonini, C., Corti, C., Peccatori, J., Castagna, A., Ciceri, F., Greco, R., 2023. Case Report: favorable outcome of allogeneic hematopoietic stem cell transplantation in SARSCoV2 positive recipient, risk-benefit balance between infection and leukemia. Front. Immunol. 14, 1184956.

Puelles, V.G., Lutgehetmann, M., Lindenmeyer, M.T., Sperhake, J.P., Wong, M.N., Allweiss, L., Chilla, S., Heinemann, A., Wanner, N., Liu, S., Braun, F., Lu, S., Pfefferle, S., Schröder, A.S., Edler, C., Gross, O., Glatzel, M., Wichmann, D., Wiech, T., Kluge, S., Pueschel, K., Aepfelbacher, M., Huber, T.B., 2020. Multiorgan and renal tropism of SARS-CoV-2. N. Engl. J. Med. 383, 590–592.

Puhach, O., Meyer, B., Eckerle, I., 2023. SARS-CoV-2 viral load and shedding kinetics. Nat. Rev. Microbiol. 21, 147–161.

Rangu, R., Wander, P.L., Zraika, S., 2022. Does diabetes risk after SARS-CoV-2 infection depend on the viral variant? Diabetes Res. Clin. Pract. 191, 110054.

Santus, P., Radovanovic, D., Saderi, L., Marino, P., Cogliati, C., De Filippis, G., Rizzi, M., Franceschi, E., Pini, S., Giuliani, F., Del Medico, M., Nucera, G., Valenti, V., Tursi, F., Sotgiu, G., 2020. Severity of respiratory failure at admission and in-hospital mortality in patients with COVID-19: a prospective observational multicentre study. BMJ Open 10, e043651.

Serreze, D.V., Wasserfall, C., Ottendorfer, E.W., Stalvey, M., Pierce, M.A., Gauntt, C., O'donnell, B., Flanagan, J.B., Campbell-Thompson, M., Ellis, T.M., Atkinson, M.A., 2005. Diabetes acceleration or prevention by a coxsackievirus B4 infection: critical requirements for both interleukin-4 and gamma interferon. J. Virol. 79, 1045–1052.

Shah, B.R., Hux, J.E., 2003. Quantifying the risk of infectious diseases for people with diabetes. Diabetes Care 26, 510–513.

Shuai, H., Chan, J.F., Hu, B., Chai, Y., Yuen, T.T., Yin, F., Huang, X., Yoon, C., Hu, J.C., Liu, H., Shi, J., Liu, Y., Zhu, T., Zhang, J., Hou, Y., Wang, Y., Lu, L., Cai, J.P., Zhang, A.J., Zhou, J., Yuan, S., Brindley, M.A., Zhang, B.Z., Huang, J.D., To, K.K., Yuen, K.Y., Chu, H., 2022. Attenuated replication and pathogenicity of SARS-CoV-2 B.1.1.529 Omicron. Nature 603, 693–699.

Shuai, H., Chan, J.F., Hu, B., Chai, Y., Yoon, C., Liu, H., Liu, Y., Shi, J., Zhu, T., Hu, J.C., Hu, YF., Hou, Y., Huang, X., Yuen, T.T., Wang, Y., Zhang, J., Xia, Y., Chen, L.L., Cai, J.P., Zhang, A.J., Yuan, S., Zhou, J., Zhang, B.Z., Huang, J.D., Yuen, K.Y., To, K.K., Chu, H., 2023. The viral fitness and intrinsic pathogenicity of dominant SARS-CoV-2 Omicron sublineages BA.1, BA.2, and BA.5. EBioMedicine 95, 104753.

Sia, S.F., Yan, L.M., Chin, A.W.H., Fung, K., Choy, K.T., Wong, A.Y.L., Kaewpreedee, P., Perera, R., Poon, L.L.M., Nicholls, J.M., Peiris, M., Yen, H.L., 2020. Pathogenesis and transmission of SARS-CoV-2 in golden hamsters. Nature 583, 834–838.

Singh, A.K., Khunti, K., 2022. COVID-19 and diabetes. Annu. Rev. Med. 73, 129–147.

Sun, S.H., Gu, H.J., Cao, L., Chen, Q., Ye, Q., Yang, G., Li, R.T., Fan, H., Deng, Y.Q., Song, X.P., Qi, Y., Li, M., Lan, J., Feng, R., Guo, Y., Zhu, N., Qin, S., Wang, L., Zhang, Y.F., Zhou, C., Zhao, L., Chen, Y., Shen, M., Cui, Y., Yang, X., Wang, X., Tan, W, Wang, H., Wang, X, Qin, C.F., 2021. Characterization and structural basis of a lethal mouse-adapted SARS-CoV-2. Nat. Commun. 12, 5654.

Tang, X., Uhl, S., Zhang, T., Xue, D., Li, B., Vandana, J.J., Acklin, J.A., Bonnycastle, L.L., Narisu, N., Erdos, M.R., Bram, Y., Chandar, V., Chong, A.C.N., Lacko, L.A., Min, Z., Lim, J.K., Borczuk, A.C., Xiang, J., Naji, A., Collins, F.S., Evans, T., Liu, C., tenOever, B.R., Schwartz, R.E., Chen, S., 2021. SARS-CoV-2 infection induces beta cell transdifferentiation. Cell Metab 33, 1577–1591.e7.

Tegally, H., Wilkinson, E., Giovanetti, M., Iranzadeh, A., Fonseca, V., Giandhari, J., Doolabh, D., Pillay, S., San, E.J., Msomi, N., et al., 2021. Detection of a SARS-CoV-2 variant of concern in South Africa. Nature 592, 438–443.

Toapanta, F.R., Ross, T.M., 2009. Impaired immune responses in the lungs of aged mice following influenza infection. Respir. Res. 10, 112.

Wang, D., Hu, B., Hu, C., Zhu, F., Liu, X., Zhang, J., Wang, B., Xiang, H., Cheng, Z., Xiong, Y., Zhao, Y, Li, Y, Wang, X, Peng, Z, 2020. Clinical characteristics of 138 hospitalized patients with 2019 novel coronavirus-infected pneumonia in wuhan, China. JAMA 323, 1061–1069.

Wang, X., Jiang, S., Ma, W., Zhang, Y., Wang, P., 2024. Robust neutralization of SARS-CoV-2 variants including JN.1 and BA.2.87.1 by trivalent XBB vaccine-induced antibodies. Signal Transduct. Targeted Ther. 9, 123.

Wu, C.T., Lidsky, P.V., Xiao, Y., Lee, I.T., Cheng, R., Nakayama, T., Jiang, S., Demeter, J., Bevacqua, R.J., Chang, C.A., Whitener, R.L., Stalder, A.K., Zhu, B., Chen, H., Goltsev, Y., Tzankov, A., Nayak, J.V., Nolan, G.P., Matter, M.S., Andino, R., Jackson, P.K., 2021. SARS-CoV-2 infects human pancreatic beta cells and elicits beta cell impairment. Cell Metab 33, 1565–1576.e5.

Wu, W., Wang, W., Liang, L., Chen, J., Sun, S., Wei, B., Zhong, Y., Huang, X.R., Liu, J., Wang, X., Yu, X., Lan, H.Y., 2023. SARS-CoV-2 N protein induced acute kidney injury in diabetic db/db mice is associated with a Mincle-dependent M1 macrophage activation. Front. Immunol. 14, 1264447.

Wysocki, J., Ye, M., Soler, M.J., Gurley, S.B., Xiao, H.D., Bernstein, K.E., Coffman, T.M., Chen, S., Batlle, D., 2006. ACE and ACE2 activity in diabetic mice. Diabetes 55, 2132–2139.

Xie, Y., Al-Aly, Z., 2022. Risks and burdens of incident diabetes in long COVID: a cohort study. Lancet Diabetes Endocrinol. 10, 311–321.

Yang, J.K., Feng, Y., Yuan, M.Y., Yuan, S.Y., Fu, H.J., Wu, B.Y., Sun, G.Z., Yang, G.R., Zhang, X.L., Wang, L., Xu, X., Xu, X.P., Chan, J.C., 2006. Plasma glucose levels and diabetes are independent predictors for mortality and morbidity in patients with SARS. Diabet. Med. 23, 623–628.

Zhang, Z., Zhang, N., Lu, X., Zhou, M., Yan, X., Gu, W., Yang, J., Zhang, Q., Zhang, C., Gong, Y., Jia, M., Zhang, X., Ning, P., Liu, M., Li, X., Shi, X., Liu, W., Gao, G.F., Ning, G., Wang, J., Bi, Y., 2023. Anti-infection effects of heparin on SARS-CoV-2 in a diabetic mouse model. Zool. Res. 44, 1003–1014.

Zhou, P., Yang, X.-L., Wang, X.-G., Hu, B., Zhang, L., Zhang, W., Si, H.-R., Zhu, Y., Li, B., Huang, C.-L., Chen, H.D., Chen, J., Luo, Y., Guo, H., Jiang, R.D., Liu, M.Q., Chen, Y., Shen, X.R., Wang, X., Zheng, X.S., Zhao, K., Chen, Q.J., Deng, F., Liu, L.L., Yan, B., Zhan, F.X., Wang, Y.Y., Xiao, G.F., Shi, Z.L., 2020. A pneumonia outbreak associated with a new coronavirus of probable bat origin. Nature 579, 270–273.

Zhu, N., Zhang, D.Y., Wang, W.L., Li, X.W., Yang, B., Song, J.D., Zhao, X., Huang, B.Y., Shi, W.F., Lu, R.J., et al., 2020. A novel coronavirus from patients with pneumonia in China, 2019. N. Engl. J. Med. 382, 727–733.